Indonesian Journal of Science & Technology

Journal homepage: http://ejournal.upi.edu/index.php/ijost/

Analysis of the behavior of asynchronous electric drive with a closed scalar control system when changing the inductance of the magnetizing circuit

Yu.L. Zhukovskiy[1,], B.Y. Vasilev[2], N.A. Korolev[1], Y.M. Malkova[2]*

[1]Educational Research Center for Digital Technologies, Saint Petersburg Mining University, Russia

[2]Department of Electrical Engineering, Saint Petersburg Mining University, Russia

Correspondence: E-mail: zhukovskiy_yul@pers.spmi.ru

ABSTRACT

The article was devoted to the study of an automated electric drive with a scalar closed-loop speed control system. Severe duty and operating modes of electric drive determine the actual service life. Wear of the induction motor, as a key link of the electric drive, was associated with deviation from nominal parameters. The deviation of parameters of the induction motor equivalent circuit determined the resultant change of characteristics. The parameters of the equivalent circuit determined the accuracy of the adjustment of regulators and optimal algorithms in the control system of the electric drive. In continuous operation modes the possibility of auto-tuning regulators, which requires stopping or no-load mode, was excluded. The paper considered the influence of the magnetization circuit mutual inductance value of the induction motor on the behavior of the electric drive control system. Evaluation of the behavior of the scalar closed-loop speed control system was performed on the basic energy (power factor, efficiency factor) and mechanical (speed, electromagnetic torque) characteristics of the electric drive.

ARTICLE INFO

Article History:
Submitted/Received 20 Jul 2022
First Revised 19 Sep 2022
Accepted 09 Nov 2022
First Available Online 10 Nov 2022
Publication Date 01 April 2023

Keyword:
Automatic electric drive,
Induction motor,
Parameters of equivalent circuit,
Magnetization circuit mutual inductance,
Scalar control system,
Technical condition.

1. INTRODUCTION

Existing approaches to improve efficiency in the operation of frequency-regulated electric drives of industrial machines and units are based on achieving their optimal energy and mechanical parameters. The required indicators are achieved by implementing various solutions in the power and control parts of electric drives. Recently, digital technologies have proven to be a good tool for increasing the efficiency of industrial facilities by improving the algorithms in the control systems (Runji et al., 2022; Nikolaev et al., 2022). The application of neural networks (Ewert et al., 2020; Zhou et al., 2021) and machine learning algorithms (Kudelina, 2021; Manikandan & Duraivelu, 2021) eliminates the need to solve problems of optimization of energy and mechanical parameters and provides the required quality of regulation in control systems of electric drives and typical mechanisms.

1.1. Algorithmic Approaches to Improve the Electromechanical Performance of the Asynchronous Electric Drive

A hybrid pulse-width modulation (PWM) algorithm provides a stable power factor. The application of the new type of controller with the algorithm of space vector pulse width modulation (SVPWM) in the scalar control system. Such a combination of control algorithms allows the achievement of higher output voltage while providing nominal electromechanical characteristics by maintaining nominal flux linkage at different speed ranges. The authors (Zhang & Yu, 2007; Hua, 2003) W.F. Zhang, Y.H. Yu, and B. Hua considered the effectiveness of sinusoidal pulse width modulation (SPWM) and space vector pulse width modulation (SVPWM). The effect is shown by different THD and DC voltage utilization ratio values. The choice of the appropriate modulating system must be made according to the requirements of the drive, taking these values into account. Articles by different scientific teams (Sultana et al., 2021) present the development of an experimental inverter based on FGPA (Field Programmable Gate Array-based), which provides reduction of acoustic noise and torque pulsations by implementing modulation and scalar control law.

Many scientific papers are devoted to improving the optimal control laws and finding simple and effective solutions at the stages of a startup, braking, or continuous modes of electric drive operation. For example, the Particle Swarm Optimization (PSO) and Cuckoo Search Optimization (CSO) algorithms are proposed in An algorithm by some researchers to optimize energy efficiency for scalar control of three-phase induction motors by varying the drive voltage/frequency ratio (V/F) to optimize air gap flow according to the mechanical load is proposed in (Graciola et al., 2022), resulting in 35.9% power consumption reduction in closed loop and 48.06% in open loop. Many solutions are related to bypassing resonant frequencies during acceleration (Jabłoński & Borkowski, 2022) or to reducing electromagnetic torque pulsations (Emelianov & Churkin, 2014) by including an additional stator current control loop in the scalar control system.

Adaptive algorithms of electric drive control systems are actively developed by many scientists. The main tools are fuzzy logic algorithms (Sun et al., 2009), genetic algorithms (Ustun & Demirtas, 2009), and neural network algorithms (ANN algorithms) (Krishnasamy & Ashok, 2022), which provide adjustment of regulators coefficients. A large part of scientists conducts research on an automated electric drive with a scalar control system. The choice of the control system is due to its wide application in the industry because of the low requirements for the accuracy of regulation, energy efficiency for electrical machines of low and medium power, and economic feasibility of application.

DOI: https://doi.org/10.17509/ijost.v8i1.51983
p- ISSN 2528-1410 e- ISSN 2527-8045

Asynchronous automated electric drives for fan and pump systems are common and responsible consumers in oil and gas and mining enterprises (Dokka et al., 2020; Boikov & Payor, 2022). The control of fan mechanisms is characterized by the use of a scalar control system with appropriate optimization. The article proposes to consider an asynchronous automated electric drive using a scalar control system to achieve optimal energy and mechanical parameters.

1.2. Induction Motors Deterioration and Defects

The induction motor (IM), as one of the key parts of the electric drive, is subject to multifactorial effects from the frequency converter, operating mechanism, and environment (Lavrenko & Shishljannikov, 2021; Bolobov et al., 2019). Although the squirrel-cage IM is a rather reliable machine (Marfoli et al., 2021), its operation is accompanied by wear and appearance of defects under the influence of the above factors. Defects appearing at the initial stage does not lead to emergency operation modes and a shutdown of the machine. Such failures can include:

(i) failures and interturn short circuits of stator winding (Bento et al., 2021; Pietrzak & Wolkiewicz, 2021);
(ii) failure of active steel package integrity (Ostroverkhov & Nalivaiko, 2020);
(iii) rotor bars breakage (Garcia-Calva et al., 2021; Fernandez-Cavero et al., 2021);
(iv) mechanical loosening of fasteners and couplings (Xiao et al., 2022).

According to the statistical data of oil and gas and mining companies (Koteleva et al., 2021), the reasons for the failures of induction motors are the defects shown in **Figure 1**. Existing approaches to improving efficiency, ensuring optimal dynamic and energy characteristics (Vasilyeva et al., 2021; Savard et al., 2021) as well as maintaining performance are largely based on the scalar control system of the electric drive. Analysis of research has shown the relevance of developing control algorithms for electric drive systems, taking into account the presence of defects in the IM (Sychev et al., 2022; Klyuev et al., 2021). However, the analysis and development of algorithms that take into account the change in stator magnetization inductance in the presence of an inter-turn fault have not been given due attention in the current literature. Therefore, this paper considers the hypothesis (idea) which is that when there is an inter-turn fault in the stator winding, asymmetry of phase voltages and deviation of circuit parameters from nominal values occurs. However, the presence of this defect does not lead to the response of the current and voltage protection systems, because the values of currents and voltages do not exceed the setting limits (Voronin & Nepsha, 2020).

At operation in continuous mode S1 and the absence of the transition to no-load mode at inter-turn short circuits in the stator, there is a mismatch in the regulator setting, which reduces the drive efficiency, initially achieved in the design. A simulation model was built to assess changes in the dynamic, mechanical, and energy characteristics of the electric drive in the presence of a defect. To perform the study experimentally, we obtained measurements of active and inductive impedances of an induction motor at inter-turn short circuits in the stator. Based on these measurements, the parameters of the equivalent circuit were calculated. Because of the danger of creating inter-turn short circuits and the possibility of damage to the laboratory equipment, it was decided to perform simulations of processes.

DOI: https://doi.org/10.17509/ijost.v8i1.51983
p- ISSN 2528-1410 e- ISSN 2527-8045

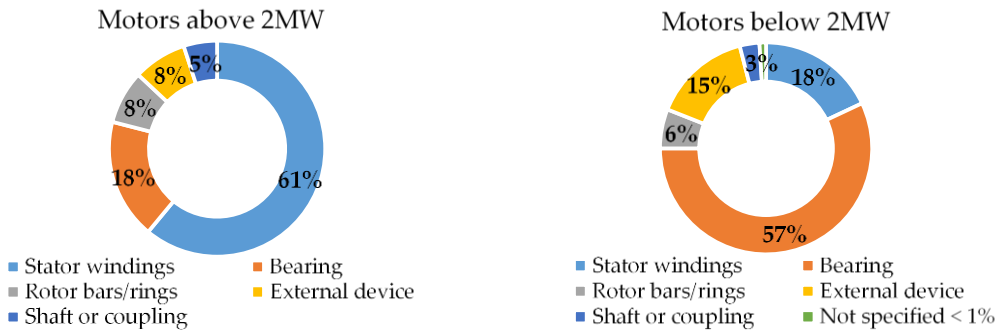

a B

Figure 1. Statistical data on the failure of asynchronous motors.

2. METHODS

The analysis of the behavior of asynchronous electric drive under the occurrence of interturn faults was carried out based on simulation modeling in Matlab Simulink in two stages: modeling of electric drive without control system; modeling of electric drive with the scalar control system.

The general structure of the investigated automated electric drive is presented in **Figure 2**. The IM is connected to the power source through a frequency converter. The power part of the inverter is represented by a two-section structure with an uncontrolled 6-pulse rectifier and a 2-level voltage inverter. The motor is controlled using a scalar closed-loop speed control system. The scalar control is carried out according to the law (1).

$$U/f=const, \quad (1)$$

where U is stator winding voltage; and f is stator winding voltage frequency.

The motor voltage on the stator windings is generated by sinusoidal PWM algorithms. In the case of modeling an electric drive without a control system, the induction motor is connected to the power source directly without a frequency converter. As the electric motor to be modeled, an IM of general industrial application AIR 315 series with nominal parameters were selected (**Table 1**). Following the passport data (**Table 1**) and measurements of IM resistance, the specified parameters of the equivalent circuit (Gridin, 2012) were calculated. The calculation results are summarized in **Table 2**.

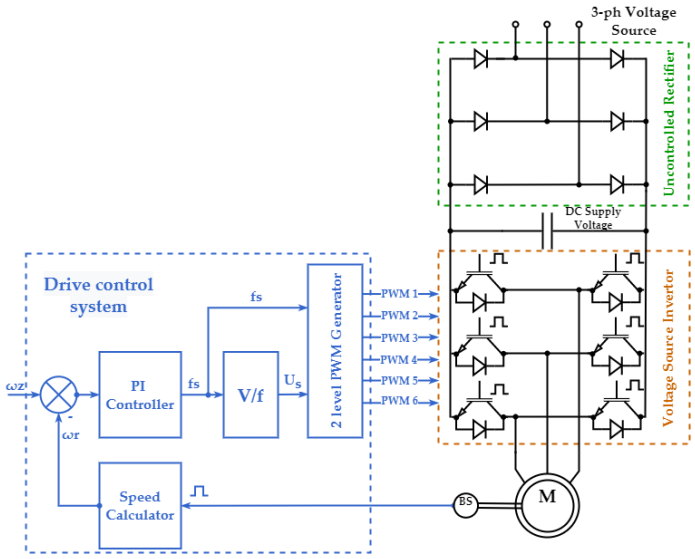

Figure 2. The structure of the scalar control system of the electric drive closed on the speed.

DOI: https://doi.org/10.17509/ijost.v8i1.51983
p- ISSN 2528-1410 e- ISSN 2527-8045

Table 1. Nominal parameters of IM.

Power P, W	Voltage Source U_n, B	Rotor speed n, rpm	Number of pole pairs z	Moment of inertia J, kg*m^2	η	cosϕ,	K_m	K_p	K_i,
132000	380	1450	2	1.5	0.9	0.86	3.0	3.0	3.0

Note: *cosφ* is the power factor; *η* is the efficiency factor; *Km* is the torque capacity; *Kp* is the starting torque ratio; and *Ki* is the starting current ratio.

Table 2. Parameters of IM equivalent circuit.

L_s H	L_r H	L_m H	R_s Om	R_r Om
0.1453	0.1473	0.1400	0.5212	0.3051

Note: *Ls* is the stator magnetization inductance, Gn; *Lr* is the rotor magnetization inductance, Gn; *Lm* is the mutual magnetization inductance, Gn; *Rs* is the stator active resistance, Ohm; and *Rr* is the rotor active resistance, Ohm.

The mathematical description of IM in fixed coordinate system αβ is represented by equations system (2), including equations of electromagnetic equilibrium, equations of currents relations with flux linkages, and equations of electromagnetic torque and motion (Vasilev, 2019):

$$\frac{d\Psi_{s\alpha}}{dt} = U_{s\alpha} - R_s I_{s\alpha}$$

$$\frac{d\Psi_{s\beta}}{dt} = U_{s\beta} - R_s I_{s\beta}$$

$$\frac{d\Psi_{r\alpha}}{dt} = -R_s I_{s\alpha} - \omega_r \psi_{r\beta}$$

$$\frac{d\Psi_{r\beta}}{dt} = -R_s I_{s\beta} + \omega_r \psi_{r\alpha}$$

$$I_{s\alpha} = \frac{1}{\sigma L_s}\Psi_{s\alpha} - \frac{k_r}{\sigma L_s}\Psi_{r\alpha} \quad (2)$$

$$I_{s\beta} = \frac{1}{\sigma L_s}\Psi_{s\beta} - \frac{k_r}{\sigma L_s}\Psi_{r\beta}$$

$$I_{r\alpha} = -\frac{k_r}{\sigma L_r}\Psi_{s\alpha} + \frac{1}{\sigma L_r}\Psi_{r\alpha}$$

$$I_{r\beta} = -\frac{k_r}{\sigma L_r}\Psi_{s\beta} + \frac{1}{\sigma L_r}\Psi_{r\beta}$$

$$M = 1.5 z L_m (I_{r\alpha} I_{s\beta} - I_{r\beta} I_{s\alpha})$$

$$\frac{d\omega_r}{dt} = \frac{M - M_c}{J}$$

where $\psi_{s\alpha}$, $\psi_{s\beta}$, $\psi_{r\alpha}$, and $\psi_{r\beta}$ are the stator and rotor flux linkage vector projections on the coordinate system axes *αβ*, Vb; $U_{s\alpha}$, $U_{s\beta}$, $U_{r\alpha}$, and $U_{r\beta}$ are the stator and rotor voltage vector projections on the coordinate system axes *αβ*, V;

$I_{s\alpha}$, $I_{s\beta}$, $I_{r\alpha}$, and $I_{r\beta}$ are the stator and rotor current vector projections on coordinate system axes *αβ*, A;

R_s and R_r are the stator and rotor active resistance, Ohm;

ω_r is the rotor speed, (rad/s);

σ is the dissipation coefficient, o.u.;

$k_s = L_m/L_s$ is the stator dissipation coefficient, o.u;

$kr = L_m/L_r$ is the rotor dissipation coefficient, o.u.

Modeling of the uncontrolled and controlled asynchronous electric drive was carried out when the magnetization circuit mutual inductance L_m was changed. Further, the estimation of energy and electromechanical parameters was performed.

3. RESULTS AND DISCUSSION

The behavior of the electric drive system was investigated when the Lm varies in the range from 0.7 to 1.1 of the nominal value with the evaluation of speed, electromagnetic torque, currents, and flux linkage at IM starting with output at nominal speed further short-term increase in nominal load (at time t = 6 c) and subsequent increase in maximum load (at time t = 7 c) in several stages.

DOI: https://doi.org/10.17509/ijost.v8i1.51983
p- ISSN 2528-1410 e- ISSN 2527-8045

Magnetization circuit mutual inductance variation in the range of 0.7-1.1-Lm is associated with interturn short currents in the frontal parts of the stator winding (Skamyin et al., 2022; Pedra et al., 2018). During the experiments, an interturn short current was created in one of the stator phases of an electric motor (**Tables 3** and **4**) having the winding stacking scheme shown in **Figure 3a**. With the help of rheostat *Rsc*, the nth number of turns in the scheme (**Figure 3b**) was closed, due to which an equivalent interturn short current was created while limiting the phase current to admissible values.

Table 3. Energy parameters of IM when changing L_m.

Parameter	Load	Lm H				
		1.1	1	0.9	0.8	0.7
Efficiency	nominal	0.9565	0.9109	0.8068	0.6249	0.40
factor	maximum	0.9565	0.9083	0.7234	0.5000	0.20
Power	nominal	0.75	0.8453	0.9031	0.8808	0.80
factor	maximum	0.9565	0.8646	0.8265	0.8000	0.78
P W	nominal	130700	145100	162800	207000	x
	maximum	203200	227500	260500	586400	x
Q VAr	nominal	60110	67160	77380	111300	x
	maximum	107700	132200	177500	574400	x
S VA	nominal	143800	159900	180200	235000	x
	maximum	230000	263100	315200	598400	x

x* is impossible to measure indicators.

Table 4. Energy parameters of the electric drive when changing L_m.

Parameter	Load	Lm H				
		1.1	1	0.9	0.8	0.7
Efficiency	nominal	x*	0.922	0.819	0.640	0.395
factor	maximum	x*	0.873	0.763	0.528	0.200
Power	nominal	x*	0.908	0.908	0.899	0.815
factor	maximum	x*	0.891	0.875	0.766	0.233
P W	nominal	x*	137400	154000	194800	300400
	maximum	x*	213000	241000	326300	658500
Q VAr	nominal	x*	63130	70770	94650	213400
	maximum	x*	108100	133000	280800	661200
S VA	nominal	x*	151200	169500	216600	368500
	maximum	x*	238900	275300	431100	679900

x* is impossible to measure indicators.

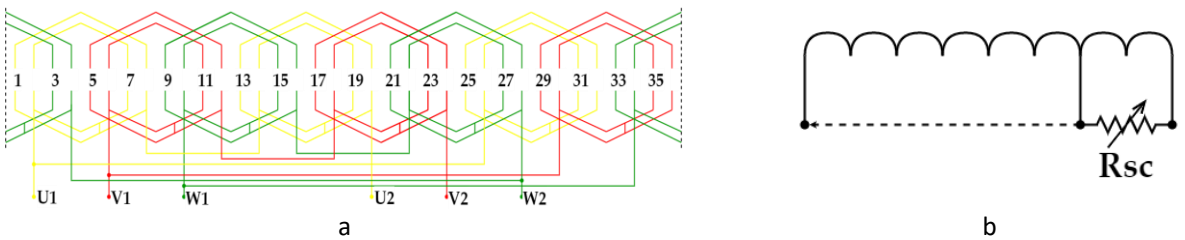

a b

Figure 3. IM AIR 315 stator: a – stator winding stacking scheme (U1; V1; W1; U1; V1; W1 – beginning and ends of phase windings); b – interturn circuit scheme.

DOI: https://doi.org/10.17509/ijost.v8i1.51983
p- ISSN 2528-1410 e- ISSN 2527-8045

The interturn short current leads to a change in the parameters of the equivalent circuit and, as a result, to a change in Lm.

3.1. Simulation of an Asynchronous Electric Drive Without a Control System

In the first stage, the simulation of an IM was performed with the formula (2) without control when powered from a sinusoidal voltage of industrial frequency of 50 Hz. At the gradual change, Lm with step ~10% electromagnetic and mechanical characteristics of the electric drive was fixed (**Figure 4**):

(i) Growth of Lm by 10% increases the acceleration rate, which is accompanied by an increase in the amplitude of the starting electromagnetic torque.

(ii) Reducing Lm by 10% leads to a doubling of the acceleration time to nominal speed, while the motor cannot form an electromagnetic torque at maximum load.

(iii) Reducing Lm by 20% results in ~5 times the acceleration time to nominal speed, while the motor cannot form electromagnetic torque under load.

(iv) Reducing Lm to 30% does not provide the formation of nominal speed and electromagnetic torque, due to the reduction of the stator torque current (**Figure 5**) and the rotor flux linkage (**Figure 6**) as a result of the weakening of the electromagnetic field in the air gap.

Energy characteristics of the unregulated electric drive were evaluated taking into account the efficiency factor (EF), power factor (PF), consumed active (P), reactive (Q), and total (S) powers (**Table 3**).

An increased value of Lm, associated with the erroneous determination of the value during commissioning parameters, leads to improved energy performance at nominal and maximum load, in particular to a reduction in power consumption P, Q, S; an increase in the efficiency factor, an increase in the power factor at maximum load (**Figure 7**). An increased value of Lm occurs if this parameter is incorrectly defined during the commissioning step of a motor. It leads to improved energy characteristics at nominal and maximum load, in particular, a reduction in power consumption P, Q, and S, an increase in efficiency, and an increase in the power factor at maximum load. When an interturn short current occurs in the stator winding, the Lm value decreases, which leads to the deterioration of the energy characteristics. As the load increases, the deterioration of energy characteristics occurs faster (**Figure 7**).

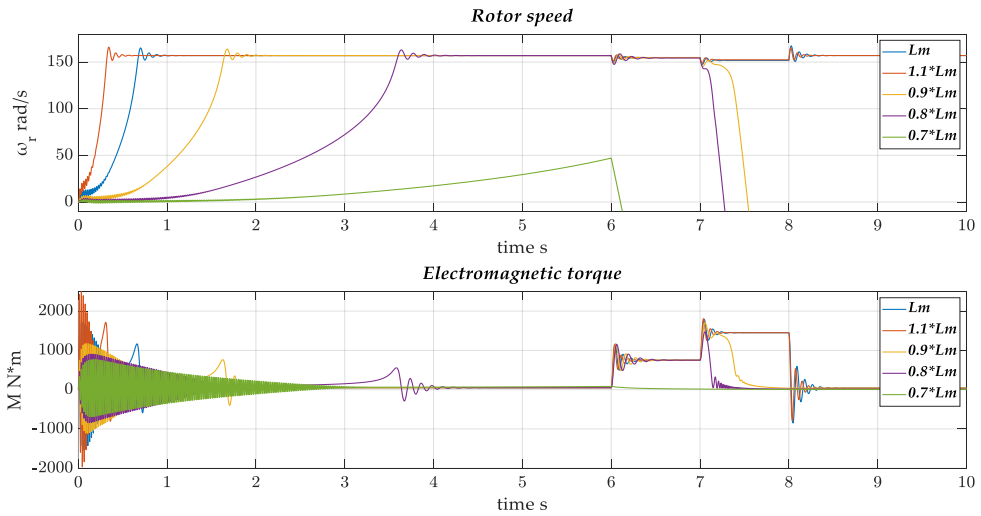

Figure 4. Rotor speed and electromagnetic torque.

DOI: https://doi.org/10.17509/ijost.v8i1.51983
p- ISSN 2528-1410 e- ISSN 2527-8045

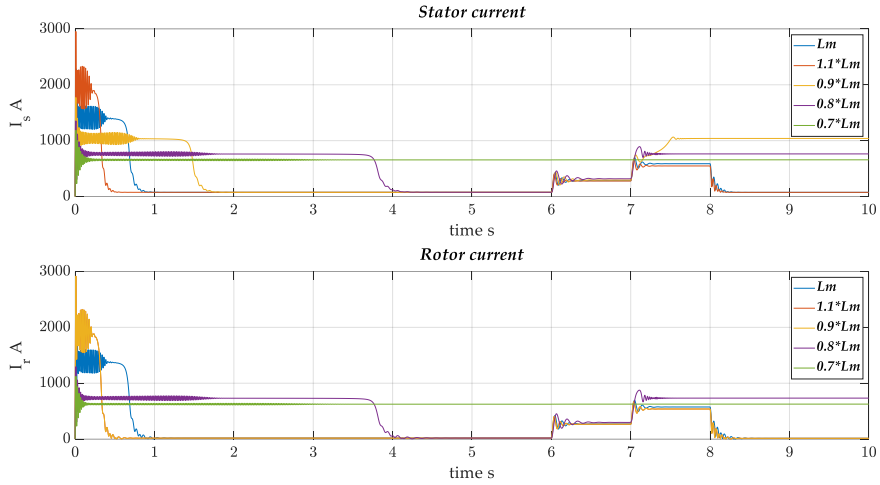

Figure 5. Stator and rotor currents.

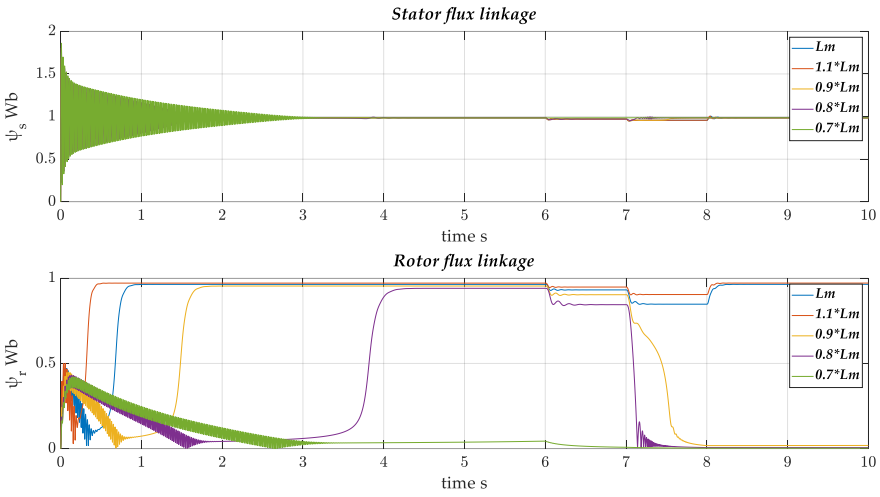

Figure 6. Stator and rotor flux linkage.

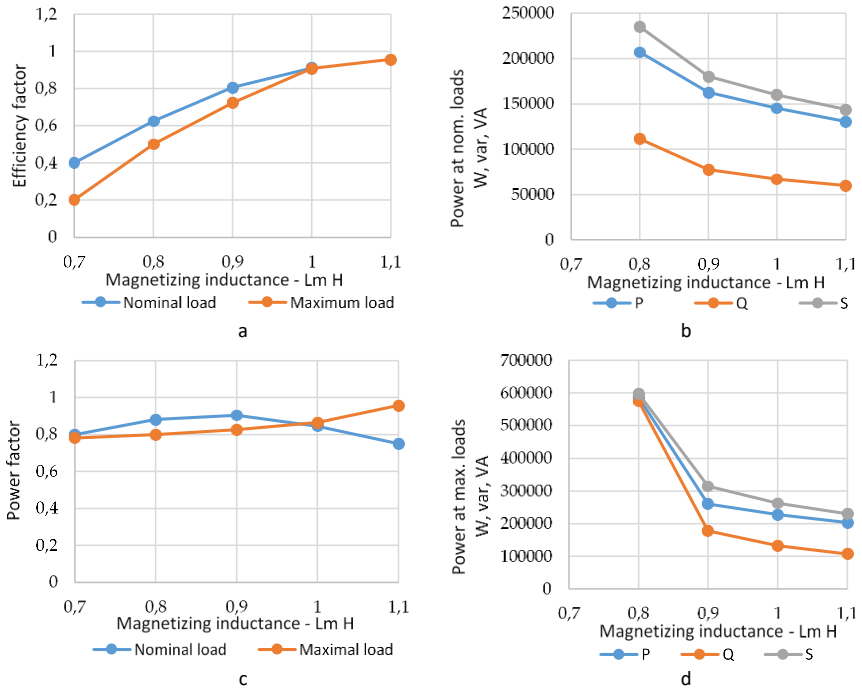

Figure 7. Energy characteristics of the electric drive when changing L_m.

DOI: https://doi.org/10.17509/ijost.v8i1.51983
p- ISSN 2528-1410 e- ISSN 2527-8045

3.2. Simulation of an Asynchronous Electric Drive with a Scalar Control System

In the second stage of simulation, the motor was powered from the frequency converter with the structure shown in **Figure 2** with a scalar closed-loop speed control system utilizing the speed sensor. Similar changes of Lm with step ~10%, as on the first stage of simulation, have led to changes in electromagnetic and mechanical characteristics of the electric drive:

(i) The rate of motor acceleration is maintained throughout the range of Lm variation, due to the closed-loop and optimal regulator tuning (**Figure 8**).

(ii) When *Lm* is reduced to 20%, the electric motor cannot generate electromagnetic torque at maximum load because of the increasing mismatch in the regulator setting and the lack of a stator current control loop.

(iii) Reducing *Lm* to 30% does not ensure the formation of the nominal electromagnetic torque, due to a decrease in stator current (**Figure 9**) and rotor flux linkage (**Figure 10**) as a result of the weakening of the electromagnetic field in the air gap.

The analysis of the energy characteristics of the controlled electric drive has similarities with the dynamics of energy characteristics decrease in the first stage of modeling (**Table 4** and **Figure 11**). However, the efficiency factor and power factor have a steeply declining characteristic as the load increases and the Lm decreases compared to the uncontrolled drive. The power consumption (**Figure 11b** and **Figure 11d**) is characterized by a smoother ramp-up over a larger range of L_m.

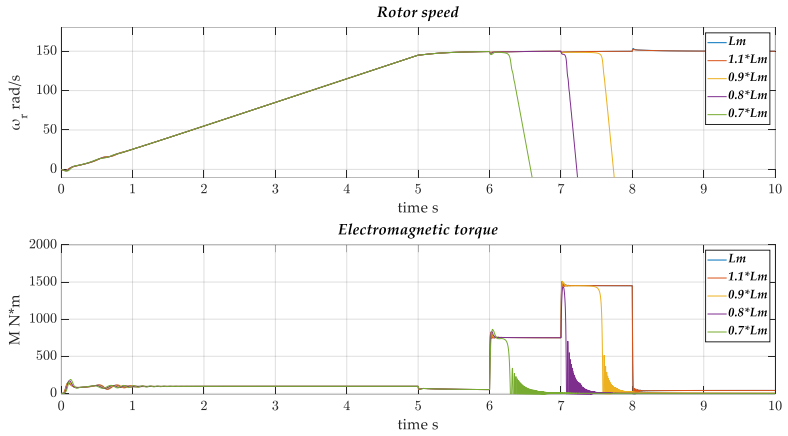

Figure 8. Rotor speed and electromagnetic torque.

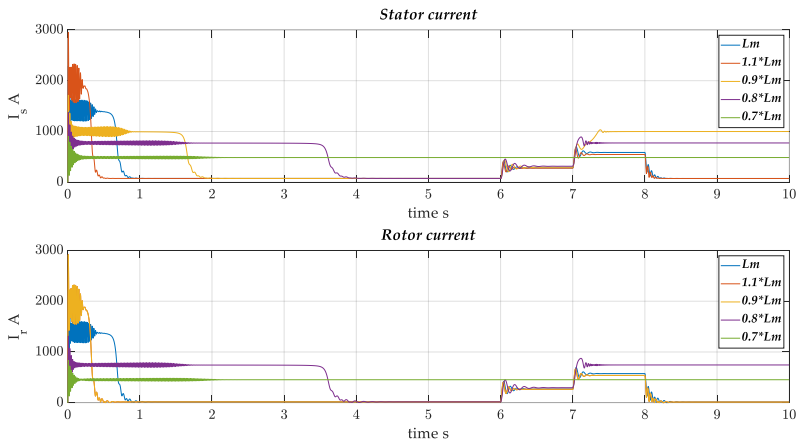

Figure 9. Stator and rotor currents.

DOI: https://doi.org/10.17509/ijost.v8i1.51983
p- ISSN 2528-1410 e- ISSN 2527-8045

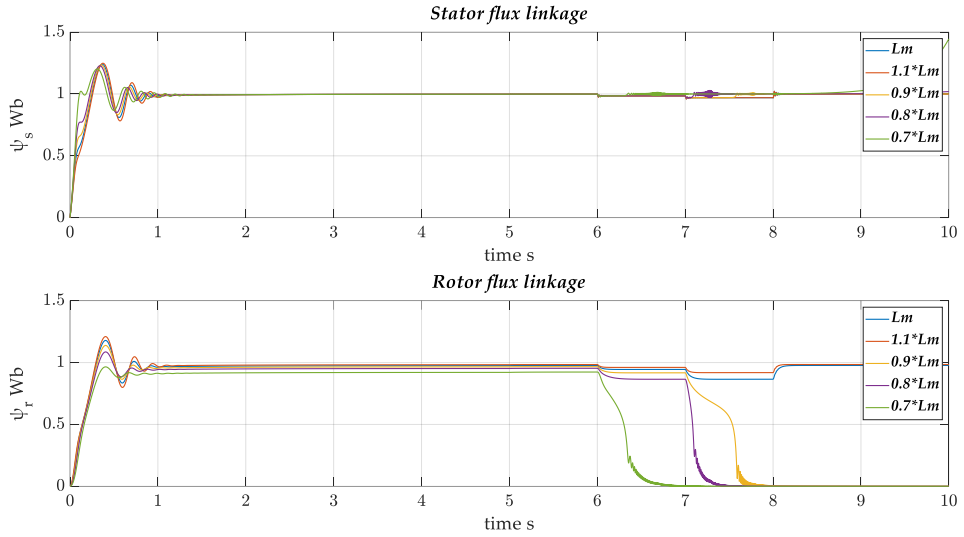

Figure 10. Stator and rotor flux linkage.

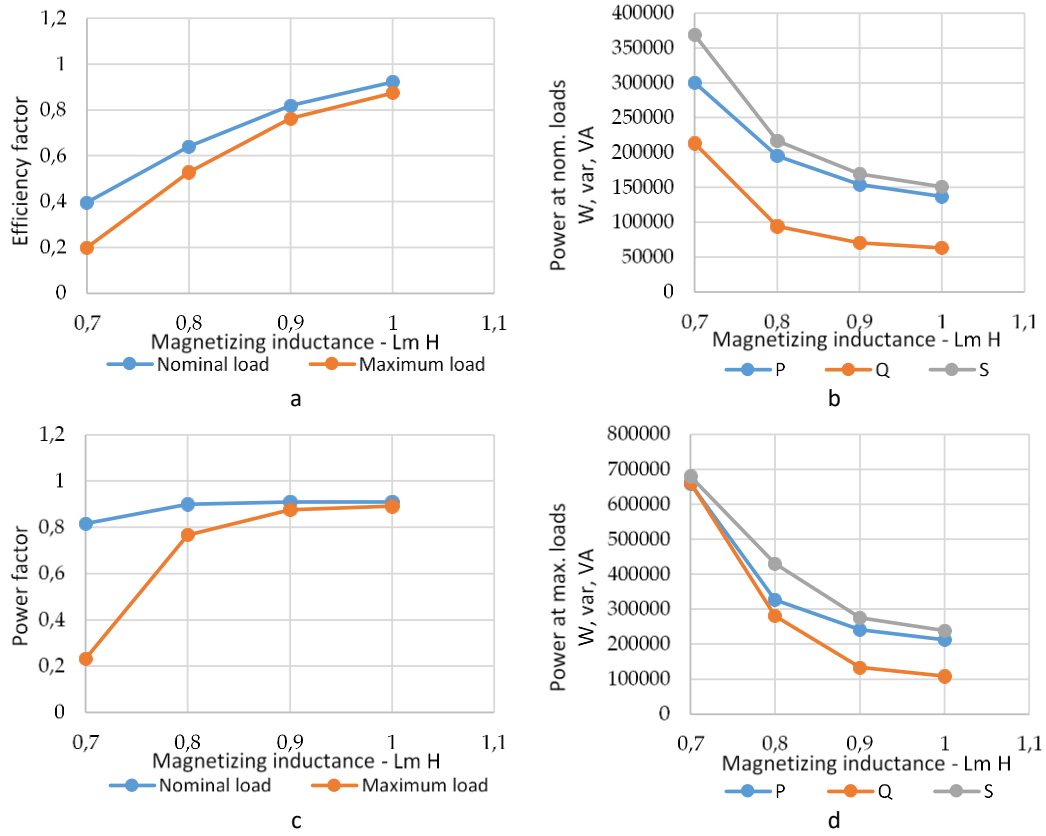

Figure 11. Energy characteristics of the electric drive when changing L_m.

4. CONCLUSION

According to the results, the simulation modeling confirmed the hypothesis about the influence of the presence and level of the defect in the form of stator interturn short current on the characteristics of the electric drive operating modes and the control system stability. The approach presented by the authors allows us to estimate dynamic, power, and mechanical characteristics in the presence of interturn faults before experimental investigations. The results of the study can be applied to further work on

DOI: https://doi.org/10.17509/ijost.v8i1.51983
p- ISSN 2528-1410 e- ISSN 2527-8045

modeling the electric drive, both with other control systems and with different types and levels of defects. At the same time, it is worth highlighting many points:

(i) The approach described by the authors allows comparing of the control system under conditions of defects or faults, which allows not only for the evaluation of the energy and mechanical characteristics of the electric drive but also for determining the permissible conditions of the required functions (maintaining the rotation speed, formation of electromagnetic torque).

(ii) Combining experimental data and simulation results allows performing research under conditions of unsafe operation of equipment at interturn short currents in the stator, which allows simulating processes of changing rotor speed, electromagnetic torque, currents, and stator and rotor flux linkages in dynamics, and evaluation results of influence on the scalar control system and electric drive.

(iii) At the operation of an electric drive with defects, on the example of interturn short current in the stator winding, expressed indirectly in the change of magnetization inductance, deterioration of mechanical and energy characteristics is observed, while currents and voltages do not exceed permissible values.

(iv) We assume that deterioration of mechanical and energy characteristics of the electric drive consists of an increasing mismatch of tuning parameters of regulators according to the value of the defect. This requires their readjustment, which in continuous operation modes (without stopping or no-load operation) is impossible to perform.

5. AUTHORS' NOTE

The authors declare that there is no conflict of interest regarding the publication of this article. The authors confirmed that the paper was free of plagiarism.

6. REFERENCES

Bento, F., Adouni, A., Muxiri, A. C., Fonseca, D. S., and Marques Cardoso, A. J. (2021). On the risk of failure to prevent induction motors permanent damage, due to the short available time-to-diagnosis of inter-turn short-circuit faults. *IET Electric Power Applications*, *15*(1), 51-62.

Boikov, A., and Payor, V. (2022). The present issues of control automation for levitation metal melting. *Symmetry*, *14*(10), 1968.

Bolobov, V. I., Chupin, S. A., Bochkov, V. S., and Mishin, I. I. (2019). Service life extension for rock cutters by increasing wear resistance of holders by thermomechanical treatment. *Journal of Mining Institute*, *5*, 67-71.

Dokka, Z., Liubov, N., and Filatova, I. (2020). Problems of oil refining industry development in Russia. *International Journal of Engineering Research and Technology*, *13*(2), 267-270.

Emelianov, A. P., and Churkin, B. A. (2014). Scalar control of squirrel-cage induction motor with stator active current. *Bulletin of the South Ural State University, Series" Power Engineering*, *14*(3), 85-90.

DOI: https://doi.org/10.17509/ijost.v8i1.51983
p- ISSN 2528-1410 e- ISSN 2527-8045

Ewert, P., Kowalski, C. T., and Orlowska-Kowalska, T. (2020). Low-cost monitoring and diagnosis system for rolling bearing faults of the induction motor based on neural network approach. *Electronics*, *9*(9), 1334.

Fernandez-Cavero, V., García-Escudero, L. A., Pons-Llinares, J., Fernández-Temprano, M. A., Duque-Perez, O., and Morinigo-Sotelo, D. (2021). Diagnosis of broken rotor bars during the startup of inverter-fed induction motors using the dragon transform and functional ANOVA. *Applied Sciences*, *11*(9), 3769.

Garcia-Calva, T. A., Morinigo-Sotelo, D., Fernandez-Cavero, V., Garcia-Perez, A., and Romero-Troncoso, R. D. J. (2021). Early detection of broken rotor bars in inverter-fed induction motors using speed analysis of startup transients. *Energies*, *14*(5), 1469.

Graciola, C. L., Goedtel, A., Angélico, B. A., Castoldi, M. F., and Costa, B. L. G. (2022). Energy efficiency optimization strategy for scalar control of three-phase induction motors. *Journal of Control, Automation and Electrical Systems*, *33*(3), 1032-1043.

Gridin, V. M. (2012). Calculation of parameters of the asynchronous motor equivalent circuit according to catalogue data. *Electricity*, *5*, 40-44.

Hua, B., Zhengming, Z., Shuo, M., Jianzheng, L., and Xiaoying, S. (2003). Comparison of three PWM strategies-SPWM, SVPWM and one-cycle control. *The Fifth International Conference on Power Electronics and Drive Systems, 2003. PEDS* 2003, *2*, 1313-1316.

Jabłoński, M., and Borkowski, P. (2022). Correction mechanism for balancing driving torques in an opencast mining stacker with an induction motor and converter drive system. *Energies*, *15*(4), 1282.

Klyuev, R. V., Golik, V. I., Bosikov, I. I., and Gavrina, O. A. (2021). Analysis of electric power loss in the power supply system of the concentrating factory. *Bulletin of the Tomsk Polytechnic University. Geo Assets Engineering*, *332*(10), 7-16.

Koteleva, N. I., Korolev, N. A., and Zhukovskiy, Y. L. (2021). Identification of the technical condition of induction motor groups by the total energy flow. *Energies*, *14*(20), 6677.

Krishnasamy, B., and Ashok, K. (2022). Assessment of harmonic mitigation in v/f drive of induction motor using an ann-based hybrid power filter for a wheat flour mill. *Processes*, *10*(6), 1191.

Kudelina, K., Vaimann, T., Asad, B., Rassõlkin, A., Kallaste, A., and Demidova, G. (2021). Trends and challenges in intelligent condition monitoring of electrical machines using machine learning. *Applied Sciences*, *11*(6), 2761.

Lavrenko, S. A., and Shishlyannikov, D. I. (2021). Performance evaluation of heading-and-winning machines in the conditions of potash mines. *Applied Sciences*, *11*(8), 3444.

Manikandan, S., and Duraivelu, K. (2021). Fault diagnosis of various rotating equipment using machine learning approaches–A review. *Proceedings of the Institution of Mechanical Engineers, Part E: Journal of Process Mechanical Engineering*, *235*(2), 629-642.

Marfoli, A., Di Nardo, M., Degano, M., Gerada, C., and Jara, W. (2021). Squirrel cage induction motor: A design-based comparison between aluminium and copper cages. *IEEE Open Journal of Industry Applications*, *2*, 110-120.

DOI: https://doi.org/10.17509/ijost.v8i1.51983
p- ISSN 2528-1410 e- ISSN 2527-8045

Nikolaev, A. V., Vöth, S., and Kychkin, A. V. (2022). Application of the cybernetic approach to price-dependent demand response for underground mining enterprise electricity consumption. *Journal of Mining Institute*, *000*, 1-10.

Ostroverkhov, V. V., and Nalivaiko, N. V. (2020). Condition assessment and diagnostics of asynchronous electric motors using signature analysis of consumed current. *Russian Electrical Engineering*, *91*(11), 714-723.

Pedra, J. (2008). On the determination of induction motor parameters from manufacturer data for electromagnetic transient programs. *IEEE Transactions on Power Systems*, *23*(4), 1709-1718.

Pietrzak, P., and Wolkiewicz, M. (2021). On-line detection and classification of PMSM stator winding faults based on stator current symmetrical components analysis and the KNN algorithm. *Electronics*, *10*(15), 1786.

Runji, J. M., Lee, Y. J., and Chu, C. H. (2022). User requirements analysis on augmented reality-based maintenance in manufacturing. *Journal of Computing and Information Science in Engineering*, *22*(5), 050901.

Savard, C., Iakovleva, E., Ivanchenko, D., and Rassõlkin, A. (2021). Accessible battery model with aging dependency. *Energies*, *14*(12), 3493.

Skamyin, A., Shklyarskiy, Y., Dobush, I., Dobush, V., Sutikno, T., and Jopri, M. H. (2022). An assessment of the share contributions of distortion sources for various load parameters. *International Journal of Power Electronics and Drive Systems*, *13*(2), 950-959.

Sultana, B., Scicluna, K., Attard, J., Seguna, C., and Scerri, J. (2021). Design of a FPGA-based inverter drive for hf injection based sensorless control. *2021 22nd IEEE International Conference on Industrial Technology (ICIT)*, 1, 178-183.

Sun, X. D., Koh, K. H., Yu, B. G., and Matsui, M. (2009). Fuzzy-logic-based V/f control of an induction motor for a DC grid power-leveling system using flywheel energy storage equipment. *IEEE Transactions on Industrial Electronics*, *56*(8), 3161-3168.

Sychev, Y. A., Aladin M. E., and Serikov, V. A. (2022). Developing a hybrid filter structure and a control algorithm for hybrid power supply. *International Journal of Power Electronics and Drive Systems*, *13*(2), 1625-1634.

Ustun, S. V., and Demirtas, M. (2009). Modeling and control of V/f controlled induction motor using genetic-ANFIS algorithm. *Energy Conversion and Management*, *50*(3), 786-791.

Vasilev, B. (2019). Analysis and improvement of the efficiency of frequency converters with pulse width modulation. *International Journal of Electrical and Computer Engineering*, *9*(4), 2314.

Vasilyeva, N. V., Boikov, A. V., Erokhina, O. O., and Trifonov, A. Y. (2021) Automated digitization of radial charts. *Journal of Mining Institute* , *247*, 82-87.

Voronin, V. A., and Nepsha, F. S. (2020). Simulation of the electric drive of the shearer to assess the energy efficiency indicators of the power supply system. *Journal of Mining Institute*, *246*, 633-639.

DOI: https://doi.org/10.17509/ijost.v8i1.51983
p- ISSN 2528-1410 e- ISSN 2527-8045

Xiao, L., Xu, Y., Sun, X., Xu, H., and Zhang, L. (2022). Experimental investigation on the effect of misalignment on the wear failure for spline couplings. *Engineering Failure Analysis*, *131*, 105755.

Zhang, W. F., and Yu, Y. H. (2007). Comparison of three SVPWM strategies. *Journal of Electronic Science and Technology*, *5*(3), 283-287.

Zhou, X., Mao, S., and Li, M. (2021). A novel anti-noise fault diagnosis approach for rolling bearings based on convolutional neural network fusing frequency domain feature matching algorithm. *Sensors*, *21*(16), 5532.

DOI: https://doi.org/10.17509/ijost.v8i1.51983
p- ISSN 2528-1410 e- ISSN 2527-8045